

Template-constrained macrocyclic peptides prepared from native, unprotected precursors

Kenneth V. Lawson, Tristan E. Rose, and Patrick G. Harran¹

Department of Chemistry and Biochemistry, University of California, Los Angeles, CA 90095

Edited* by Kendall N. Houk, University of California, Los Angeles, CA, and approved August 26, 2013 (received for review June 19, 2013)

Peptide–protein interactions are important mediators of cellular-signaling events. Consensus binding motifs (also known as short linear motifs) within these contacts underpin molecular recognition, yet have poor pharmacological properties as discrete species. Here, we present methods to transform intact peptides into stable, templated macrocycles. Two simple steps install the template. The key reaction is a palladium-catalyzed macrocyclization. The catalysis has broad scope and efficiently forms large rings by engaging native peptide functionality including phenols, imidazoles, amines, and carboxylic acids without the necessity of protecting groups. The tunable reactivity of the template gives the process special utility. Defined changes in reaction conditions markedly alter chemoselectivity. In all cases examined, cyclization occurs rapidly and in high yield at room temperature, regardless of peptide composition or chain length. We show that conformational restraints imparted by the template stabilize secondary structure and enhance proteolytic stability in vitro. Palladium-catalyzed internal cinnamylation is a strong complement to existing methods for peptide modification.

Synthetic peptides and peptidomimetics play wide-ranging roles in pharmacology and drug discovery. Interest in these substances continues to grow, particularly as medicinal chemistry pushes further into control of cellular-signaling events mediated by protein–protein interactions (PPIs) (1–3). The subset of so-called “druggable” PPIs includes those mediated by consensus peptides, where binding determinants are localized within defined motifs (4–8). Experimental data as well as computational/bioinformatic efforts (9–11) to identify “short linear motifs” within signaling proteins suggest that the number of druggable PPIs has been underestimated (12, 13). Considerable opportunity exists for new chemistry in this area (14). Synthetic peptides that target “hot spots” on protein surfaces are a logical entry to drug-discovery programs (15–19). However, native peptides generally have poor pharmacological properties (20). Modifications that offset those limitations while stably recapitulating protein-binding conformations are of considerable interest (14, 21–23).

Ring-forming reactions are prominent among alterations found to improve the stability and performance of peptides (24–27). They find broad utility in synthesis and, increasingly, in combination with phage, ribosome, and mRNA display technologies (28–32). Relative to their acyclic counterparts, cyclic peptides have more defined conformations and are less prone to aggregate (33). Head-to-tail lactamization is the most common method to synthesize cyclic peptides (34–36). Internal disulfide bonding is also used (37, 38), as are newer techniques such as ring-closing olefin metathesis (39) and catalyzed cycloaddition of azides to alkynes (40–42). These procedures rely on judicious use of protecting groups and/or tailored amino acid residues (Fig. 1A) (43, 44). Careful attention must be paid to substrate conformational biases to avoid competing oligomerization. Moreover, lactamization of peptides shorter than five residues can be particularly difficult (34, 45).

An alternate method to incorporate short epitopes into rings is through the use of scaffolds. Degradó and coworkers (46), Boger and Myers (47), and others have shown the utility of such template-constrained cyclic peptides (48, 49), and how polarity and

geometry of the template can influence the shape and function of the peptide domain (50). Our laboratory has also explored templates for forming macrocyclic peptides (51–53). In this work, templates were designed as multiply reactive inserts. Stepwise engagement with a variety of peptides gave unique composite products. The resultant structures varied in shape, possessed defined conformations, and increased solubility.

The large ring-forming reaction in these processes was an allylic substitution catalyzed by palladium(0). We observed that decomposition of a cinnamyl carbonate within the template could capture pendant tyrosine residues to form cyclic ethers (51, 54). This result followed from catalysis pioneered by Tsuji and Trost. Palladium-catalyzed substitution of allylic leaving groups (also known as the “Tsuji–Trost reaction”) is a versatile and well-studied process (55, 56). Mechanistically, it involves intermediate palladium π -allyl complexes that function as electrophiles. The chemistry occurs under mild conditions and is amenable to ligand-induced regio- and stereocontrol. It has been applied broadly, including in numerous instances to form large carbocyclic and heterocyclic rings (57–60). That said, when we simplified our templates to further study the catalysis in the context of cyclic-peptide synthesis, we discovered a combination of scope and functional group tolerance that was remarkable. We describe those results here.

We show that intramolecular palladium-catalyzed cinnamylation of heteroatom nucleophiles can operate within highly functionalized native peptides. The nucleophile in the macrocyclization can be an amine, a carboxylic acid, a phenol, an imidazole, or an aniline. Chemoselectivity is predictable and in many cases switchable. With one exception (see *Results and Discussion*), the reaction is catalyzed by a commercial complex of palladium(0), namely Pd(PPh₃)₄. No exotic or costly ligand sphere for the metal is necessary. No protecting groups are used in any substrate. Reactions proceed rapidly and in high yield at room

Significance

Cyclic peptides and peptidomimetics are valuable tools in biomedical research. This paper describes chemistry to convert linear, unmodified peptides directly into stable, templated macrocycles. The ring-closing reaction is an allylic substitution catalyzed by palladium(0). It requires no tailored amino acid residues or protecting groups. It proceeds rapidly at room temperature and largely independent of product-ring size and composition. The catalysis shows broad scope and predictable chemoselectivity while engaging functional groups native to peptides. These methods could be applied broadly and have special utility for those attempting to perturb biological systems with unique small molecules.

Author contributions: K.V.L., T.E.R., and P.G.H. designed research; K.V.L. and T.E.R. performed research; and K.V.L., T.E.R., and P.G.H. wrote the paper.

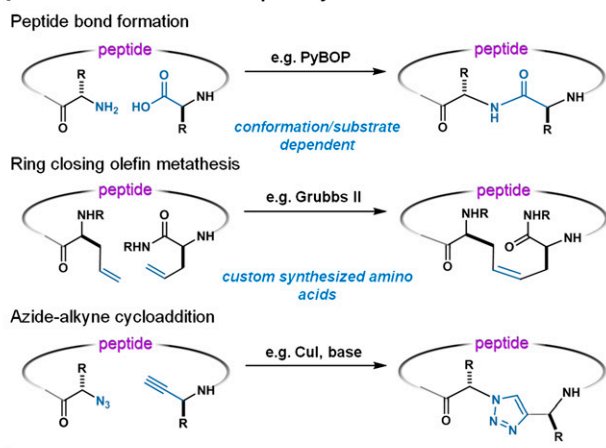
The authors declare no conflict of interest.

*This Direct Submission article had a prearranged editor.

¹To whom correspondence should be addressed. E-mail: Harran@chem.ucla.edu.

This article contains supporting information online at www.pnas.org/lookup/suppl/doi:10.1073/pnas.1311706110/-DCSupplemental.

A Established Methods for Peptide Cyclization:



B Current Work: Templated Macrocyclization Catalyzed by Palladium(0)

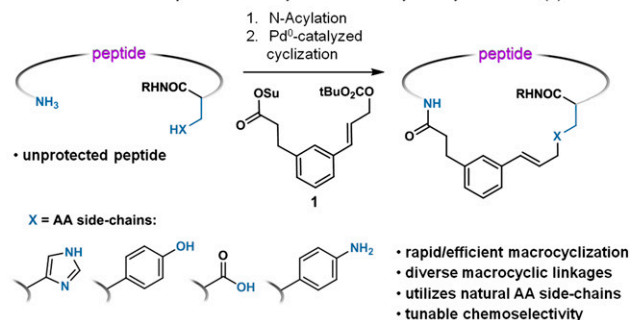


Fig. 1. (A) Existing methods for peptide cyclization can be sensitive to substrate conformational preferences and/or require tailored amino acid residues. (B) The template-based cyclizations described here are catalyzed allylic substitutions. They engage native peptide functionality and proceed largely independent of oligomer length and composition.

temperature and, thus far, independent of product-ring size and composition.

Results and Discussion

Template **1** (Fig. 1B) is reminiscent of a lignan monomer. It is a simplified, achiral form of a structure we described previously (51). The intent was to study large ring-forming reactions involving palladium π -allyl intermediates generated from the cinnamyl carbonate in this molecule. Compound **1** was synthesized in six steps and 51% overall yield from commercial 3-(3-bromophenyl)propionic acid (*SI Appendix*, Fig. S2). Multigram batches of solid **1** were prepared and stored at room temperature without incident. Procedures using this material were designed to be simple. Its active ester acylated peptidyl amines in neutral *N,N*-dimethylformamide (DMF) at room temperature. The resultant adducts reacted with catalytic amounts of commercial Pd(PPh₃)₄ in argon-sparged DMF, also at room temperature.

Initial experiments served to probe catalyzed cycloetherification of tyrosine residues (Fig. 1B, XH = PhOH). Attention focused on how ring size, solvent, additives, and substrate concentration affected reaction rate and efficiency. As these experiments progressed, we observed a much greater functional group tolerance than expected. Moreover, residues such as aspartic acid, glutamic acid, and histidine would participate as nucleophiles in the cyclization, as would a free carboxyl or amino terminus under appropriate conditions. Chemoselectivity was both predictable and tunable. In two steps, beginning with **1** and an unprotected peptide, we could achieve any one of several cyclization modes including head-to-tail, side chain-to-tail, and side chain-to-side

chain. Peptides up to 11 residues long were readily transformed into templated macrocycles.

Impact of Solvent, Substrate Concentration, and Base Additives on Catalyzed Cycloetherification of Tyrosyl Phenols. Linear substrate **2** (Fig. 2A) was chosen to evaluate affects of solvent and additives on catalyzed internal etherification of its tyrosyl phenol. N-acylation of synthetic Ala-Trp-Thr-Tyr with *N*-hydroxysuccinidyl ester **1** gave adduct **2** in 72% yield. Exposure of **2** to 5 mol % Pd(PPh₃)₄ in deoxygenated DMF (5 mM in **2**) at room temperature caused rapid conversion to cyclic ether **4** in 91% HPLC assay yield (78% when isolated by preparative HPLC). Reaction monitoring showed complete conversion to product within 15 min (Fig. 2B). No dimeric or oligomeric materials were detected in the experiment. As illustrated in Fig. 2D, the catalysis proceeded efficiently in several polar aprotic solvents. The use of water as cosolvent was tolerated (entry 5), but it slowed the reaction rate ~30-fold and resulted in formation of an unidentified side-product (~15%).

In neat DMF, contact ion pairing of transient intermediates within the catalytic cycle may explain the rapid reaction rate and high product yield (61, 62). Consistent with literature precedent, *tert*-butoxide formed from decomposition of the cinnamyl carbonate following oxidative addition of Pd⁰ to the allylic C–O sigma bond likely deprotonates the proximal phenol, resulting in a new, more product-like (i.e., cyclic, Fig. 2C) metal ion pair. Reductive elimination or displacement of palladium would follow, leading to product. Electrostatic preorganization of amphoteric peptides has been discussed previously (63, 64). The inner salts invoked here as intermediates formed at low concentration would likewise be expected to offset entropic costs associated with ring formation (64, 65). It is also consistent with a general lack of oligomeric products formed in the catalysis, which can limit other peptide cyclization methods (45, 66, 67). High macrocyclization efficiency (calculated Emac index = 7.77) (68) was observed at 20-fold higher concentration (0.1 M), wherein the isolated yield was lowered only slightly (Fig. 2D, entry 2).

When cinnamyl acetate **3** (Fig. 2A) was subjected to identical cyclization conditions, conversion to **4** was not observed even upon prolonged heating (Fig. 2D, entry 6). We speculated that, unlike the situation for **2**, acetate ion liberated by oxidative addition of Pd⁰ to **3** was insufficiently basic to propagate a catalytic cycle involving a tyrosyl phenoxide. Consistent with this hypothesis, addition of Cs₂CO₃ (2 equiv., Fig. 2D, entry 7) rescued the reaction, promoting rapid conversion of **3** to cinnamyl ether **4**. Under buffered aqueous conditions, the cyclization rate was pH dependent. No conversion of **2** to **4** was observed when an equal mixture of DMF and pH 5.5 phosphate buffer was used as solvent (entry 8). Increasing the buffer pH to 7.4 induced a sluggish reaction. Complete conversion to **4** required 16 h. However, at pH 8.5 the reaction was complete within 2 h and **4** was formed in 89% HPLC assay yield. Taken together, data in Fig. 2D suggested 5 mM solutions of carbonate substrate in neat DMF (no additives) would be the most convenient to further evaluate the scope of the macrocyclization. Substrate solubility and reaction rate would be generally highest.

Evaluating the Scope of Catalyzed Cycloetherification. To define the range of macrocycles available through catalyzed cinnamylation of phenols, a set of unprotected, L-amino acid-derived peptides were prepared as C-terminal carboxamides. Peptides ranged from three to five residues long and each possessed a free amino terminus and a tyrosine residue in the sequence. All functional groups present in natural amino acids were represented in the set, with the exception of thiols (cysteine) to avoid complications from oxidative lability.

Acylation of each peptide with template **1** was achieved by mixing in DMF in the presence of (i-Pr)₂NEt (*SI Appendix*,

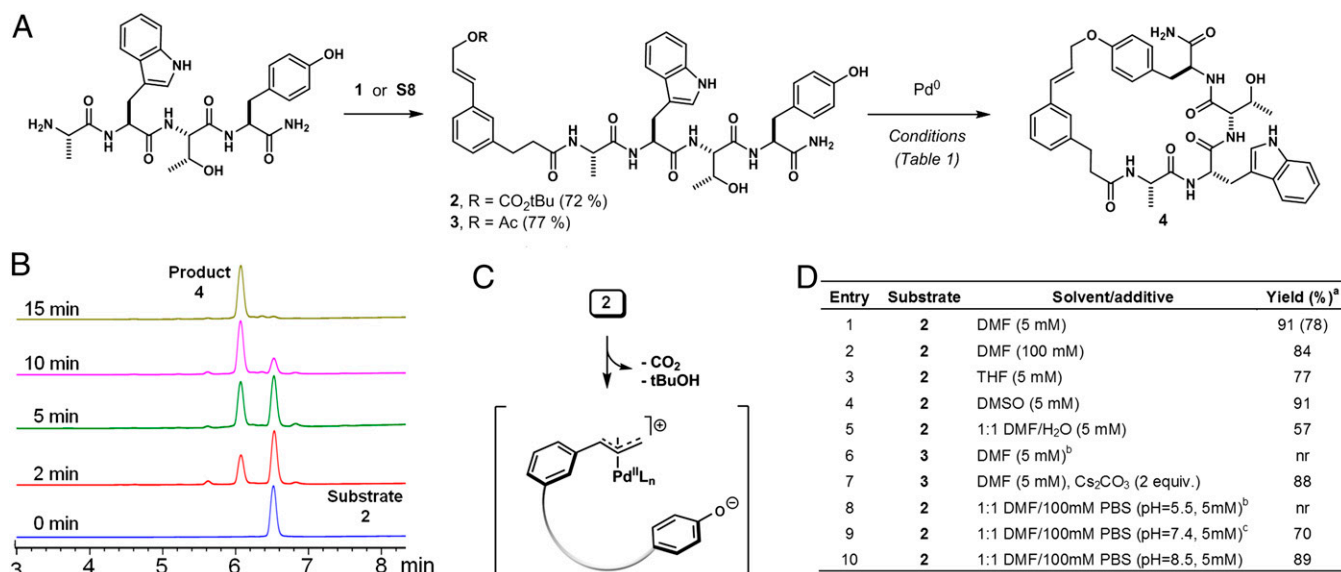


Fig. 2. (A) Catalyzed cycloetherification of substrates derived from templates **1** or **S8** and model peptide Ala-Trp-Thr-Tyr. (B) HPLC analyses (C18, 40→100% MeCN/H₂O 0.1%TFA, 10 min, monitoring at 254 nm) of samples taken from reaction of **2** with 5 mol % Pd(PPh₃)₄ (Table in D, entry 1) at the indicated time points. (C) Partial schematic of internally ion-paired π -allyl palladium(II) complex putatively generated from **2** via oxidative addition of Pd(0). (D) Media and additive effects on the palladium-catalyzed synthesis of macrocyclic ether **4** from precursors **2** and **3**. Reactions were run for 2 h at room temperature in argon sparged media containing 5 mol % Pd(PPh₃)₄. ^aYield determined by HPLC assay. Isolated yield in parentheses. ^bNo conversion at 16 h. ^c16 h reaction time. PBS, phosphate buffered solution; nr, no reaction.

Table S1). Treatment of these products with 5 mol % Pd (PPh₃)₄ gave macrocyclic cinnamyl ethers **5–9** and **11–14** (Table 1) in high isolated yields (72–85%). No branched phenylallyl ethers were detected in these experiments. Polar functional groups including alcohols, amides, and guanidines were well-tolerated. Notably, efficient macroetherification was not restricted to tyrosine. 5-Hydroxyindole, incorporated as commercial 5-hydroxytryptamine, was equally competent as a nucleophile, affording

macrocyclic ether **10** in 75% yield. For each product, the macrocyclic ether linkage was assigned by NMR, wherein a diagnostic heteronuclear multiple bond correlation (HMBC) between the cinnamyl methylene protons and the phenolic carbon resonance ($\sim \delta$ 155 ppm) was observed.

When the sequence Ala-Leu-Glu-Tyr was acylated with **1** and the product (**15**, Fig. 3A) treated with Pd(PPh₃)₄, HMBC analysis of the resultant product did not reveal the anticipated cinnamyl

Table 1. Macrocyclic ethers obtained in two steps from template **1** and the indicated unprotected peptides (listed above product)

Ser-Met-Tyr	Ile-Trp-Tyr	Ala-Val-Tyr	Trp-Ile-Gln-Tyr	Val-Met-Phe-Tyr
5 (80 %)	6 (72 %)	7 (78 %)	8 (81 %)	9 (73 %)
Gly-Thi-Trp-5HTA	Leu-Ala-Arg-Tyr	Ile-Met-Ser-Tyr-Trp	Ala-Phe-Thr-Ile-Tyr	Gly-Ser-Phe-Asn-Tyr
10 (75 %)	11 (84 %)	12 (73 %)	13 (85 %)	14 (74 %)

Isolated yield of palladium-catalyzed cyclization step indicated in parentheses. For conditions, see Fig. 2D, entry 1. 5HTA, 5-hydroxytryptamine.

A Retrosynthetic analysis of macrocyclic peptides **16** and **17**. Linear precursor **15** is cyclized to **16** using $\text{Pd}(\text{PPh}_3)_4$ in DMF (67% yield, >20:1 ratio). Linear precursor **18** is cyclized to **17** using $\text{Pd}(\text{PPh}_3)_4$ in DMF (76% yield, >20:1 ratio) and Cs_2CO_3 in DMF. The structures of **16** and **17** are shown with atom numbering for NMR assignment.

B ^1H NMR spectra of **16** (a), **17** (b), and a mixture of **16** and **17** (c) in CDCl_3 . The x-axis represents chemical shift in ppm from 0 to 10.

C ^{13}C NMR spectra of **16** (a) and **17** (b) in CDCl_3 . The x-axis represents chemical shift in ppm from 4.5 to 120. Key peaks are labeled: H1-C2 , H1-C2' , H1-C3' , H1-C3 , H1-C25 , and H1-C20 .

D Retrosynthetic analysis of macrocyclic peptides **19** and **20**. Linear precursor **18** is cyclized to **19** using $[\text{Pd}(\text{C}_3\text{H}_5)\text{Cl}]_2$ in DMF (75% yield, >20:1 ratio) and $[\text{Pd}(\text{C}_3\text{H}_5)\text{Cl}]_2$ in xantphos/DMF (68% yield, 10.2:1 ratio). Linear precursor **18** is cyclized to **20** using $[\text{Pd}(\text{C}_3\text{H}_5)\text{Cl}]_2$ in xantphos/DMSO (68% yield, 20:1 ratio) and $[\text{Pd}(\text{C}_3\text{H}_5)\text{Cl}]_2$ in xantphos/DMSO (68% yield, 20:1 ratio). The structures of **19** and **20** are shown with atom numbering for NMR assignment.

E ^1H NMR spectra of **19** (a), **20** (b), and a mixture of **19** and **20** (c) in CDCl_3 . The x-axis represents chemical shift in ppm from 0 to 10.

F ^{13}C NMR spectra of **19** (a) and **20** (b) in CDCl_3 . The x-axis represents chemical shift in ppm from 4.6 to 115. Key peaks are labeled: H1-C28 , H1-C2 , H1-C2' , H1-C30 , H1-C3' , and H1-C22' .

ether. Rather, it indicated cyclization had formed macrolactone **16** (67% isolated yield) from cinnamylation of glutamic acid. This connectivity was assigned based on HMBC correlation between the cinnamyl methylene protons (*H1*, Fig. 3C) and Glu-C20 (δ 171.6 ppm). No other products were observed by HPLC (Fig. 3B). We were cognizant that **16** could form from **15**, yet expected this compound to be susceptible to reionization by palladium(0). However, consistent with the inertness of cinnamyl acetate **3** to $\text{Pd}(\text{PPh}_3)_4$ in the absence of base (Fig. 2D, entry 6), macrolactone **16** proved stable and isolable. Resubjecting **16** to the reaction conditions did not result in isomerization to cyclic ether **17**.

In contrast, when **15** was treated with 5 mol % Pd(PPh₃)₄ in the presence of Cs₂CO₃, macrocyclic ether **17** was formed exclusively and isolated in good yield (Fig. 3 *D* and *E*). Lactone **16** was not observable by HPLC during the course of the reaction. The absence or presence of Cs₂CO₃ was a convenient means to select for a 26-membered or 21-membered ring product. Such tunable outcomes bode well for preparing structurally distinct macrocycles from a single peptide sequence.

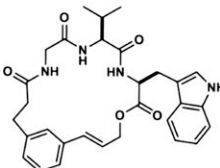
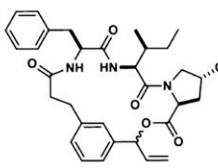
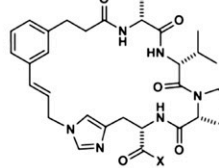
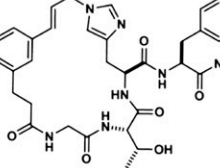
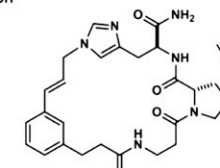
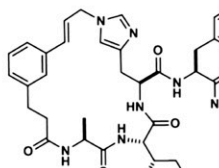
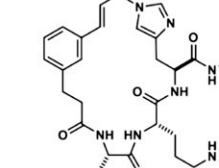
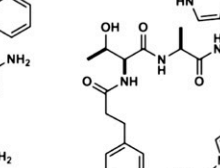
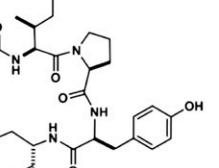
Catalyzed internal esterification proved an excellent method for head-to-tail macrolactonizations. Substrates prepared from **1** and peptides harboring a free carboxyl terminus underwent the reaction readily. For example, treatment of Gly-Val-Trp-OH and Phe-Ile-Hyp-OH with **1** followed by Pd(PPh₃)₄ efficiently produced macrolactones **21** and **22** (Table 2), respectively. Branched allylic ester **22** was isolated as a ~1:1 mixture of diastereomers. No cinnamyl linkage was detected in this instance, an atypical outcome rationalized in terms of added geometric constraints imposed by the hydroxyproline residue.

Next examined were histidine-containing substrates. Compound **18**, derived from **1** and Val-Gln-Tyr-His, was recovered unchanged after exposure to Pd(PPh₃)₄ for extended reaction times. Stable ligation of palladium by histidine-containing peptides has been reported (69–71). To mitigate suspected catalyst poisoning, we turned to a less labile/dynamic ligand sphere for the metal. When a precatalyst generated from [Pd(C₃H₅Cl)]₂ (4 mol%) and the chelating bis-phosphine xantphos (10 mol%) was used (72), complete consumption of **18** was observed within 30 min (Fig. 3E). Two regioisomeric products were obtained in an ~5:1 ratio and 75% combined yield. HMBC correlations from the cinnamyl methylene *H1* to C28 and C30 confirmed the major product as histidine N29-alkylated macrocycle **20** (Fig. 3 D and F). The minor product was determined to be its N31-alkylated regioisomer. Neutral imidazole is a weak nucleophile in solution. Direct participation of imidazoles in large ring-forming reactions is rare, yet the histidine residue was the sole site of alkylation in this reaction (73). Competition from the tyrosyl phenol was not observed. However, as observed for substrate **15**, chemoselectivity was switchable upon the addition of base.

Treatment of **18** with $[\text{Pd}(\text{C}_3\text{H}_5)_2\text{Cl}]_2/\text{xantphos}$ and Cs_2CO_3 (2 equiv.) in DMF afforded macrocyclic ether **20** in a 5.7:1 ratio relative to regioisomers **19**. Changing the reaction solvent to DMSO improved the selectivity to 10.2:1 (Fig. 3E), likely due to the increased solubility of Cs_2CO_3 in DMSO (74).

A set of peptides was prepared to examine the generality of histidine-based macrocyclization (Table 2). In each case, treatment with $[\text{Pd}(\text{C}_3\text{H}_5\text{Cl})_2]/\text{xantphos}$ afforded exclusively histidine-alkylated macrocycles in high yield. Where possible, tyrosine

Table 2. Macrocycles obtained from templated cyclization of oligomers (listed above product) containing carboxylic acids, imidazoles, and anilines

Gly-Val-Trp-OH	Phe-Ile-Hyp-OH	D-Ala-D-Val-D-Pro-His-X	Gly-Thr-His-Tyr	β -Ala-Pro(4-OAr)-His
 21 (74 %)	 22 (71 %)	 23 X = OH (69 %) 24 X = NH ₂ (77 %)	 25 (73 %)	 26 (81 %)
Ala-Ile-His-Phe	Ala-Arg-His-Phe	Thr-Ala-Trp-Ile-Pro-Tyr-His-Asn-Val	Asn-Trp-Thr-Phe(4-NH ₂)	
 27 (71 %)	 28 (76 %)	 29 (69 %)	 30 (77 %)	

Isolated yield of palladium-catalyzed cyclization step indicated in parentheses. For conditions see *SI Appendix*.

alkylation was not detected regardless of resultant ring size (e.g., **25** versus **29**). Histidine alkylation also occurred in preference to macrolactone formation in the presence of free carboxylic acids (see **23**). Other polar functional groups including amides, alcohols, and guanidines were well tolerated. Sequences containing both histidine and residues displaying primary amines (i.e., Lys or Orn) were unique in that cyclization was unselective and low yielding. Only the combination of histidine caused this result with amines, which likely could be managed using orthogonal protection schemes.

In other settings, amines were useful and competent reaction partners in Pd⁰-catalyzed cinnamylation (75). Moreover, use of the xantphos ligand was no longer necessary. For example, acylation of Fmoc-Val-Orn-Met-Tyr with template **1** followed by treatment

with piperidine gave adduct **31** (Fig. 4A). Exposure of this material to 5 mol % Pd(PPh₃)₄ resulted in exclusive cinnamylation of the amino terminus to afford **33** (>95% HPLC peak area purity). Analogous to previous examples, chemoselectivity was sensitive to added base. The addition of 3 equiv. Cs₂CO₃ and use of DMSO as solvent provided cinnamyl ether **32** as the sole cyclization product. Under the same conditions, substrate **34** derived from **1** and Orn-Thr-Tyr gave macrocyclic ether **35** in 80% yield. The primary amine and secondary alcohol were unaffected.

We next examined a third type of nitrogen nucleophile in the cyclization reaction. Sequences were prepared containing the nonproteinogenic amino acid 4-aminophenylalanine, which is readily available and used as a tyrosine isostere (76, 77). Peptides Ser-Phe-Phe(4-NH₂) and Asn-Trp-Thr-Phe(4-NH₂) were mixed

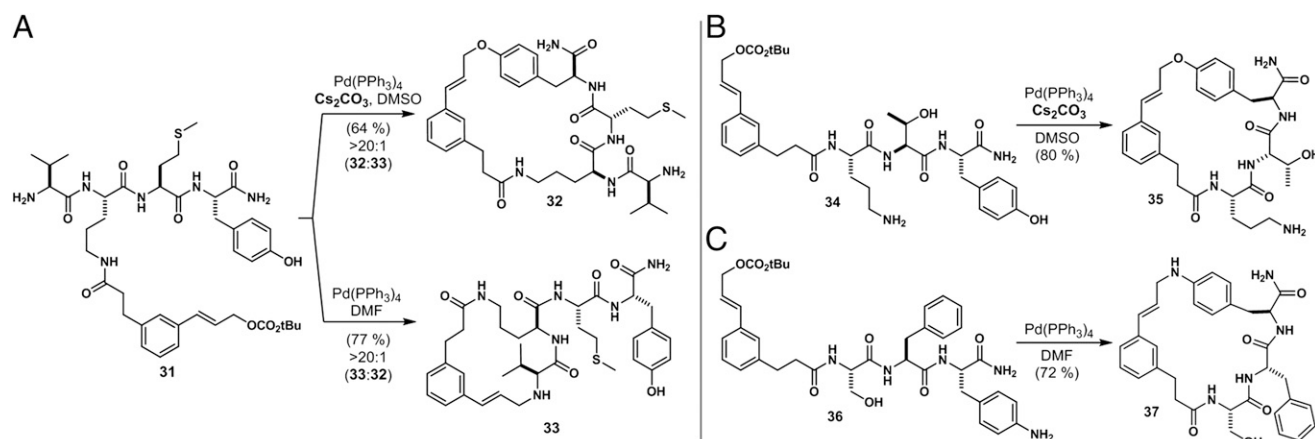


Fig. 4. (A) Cyclization chemoselectivity in a sequence containing a tyrosine residue and a free amino terminus is high and base-dependent. Conditions: For **32**, Pd(PPh₃)₄ (5 mol %), Cs₂CO₃ (3 equiv.), DMSO (5 mM in **31**); for **33**, Pd(PPh₃)₄ (5 mol %), DMF (5 mM in **31**). (B) In the presence of base, primary amines do not interfere with tyrosyl cyclizations. Conditions: Pd(PPh₃)₄ (5 mol %), Cs₂CO₃ (3 equiv.), DMSO (5 mM in **34**). (C) A sequence containing *p*-aminophenylalanine cyclizes readily in the absence of base. Conditions: Pd(PPh₃)₄ (5 mol %), DMF (5 mM in **36**). Yields in parentheses refer to material isolated by preparative HPLC.

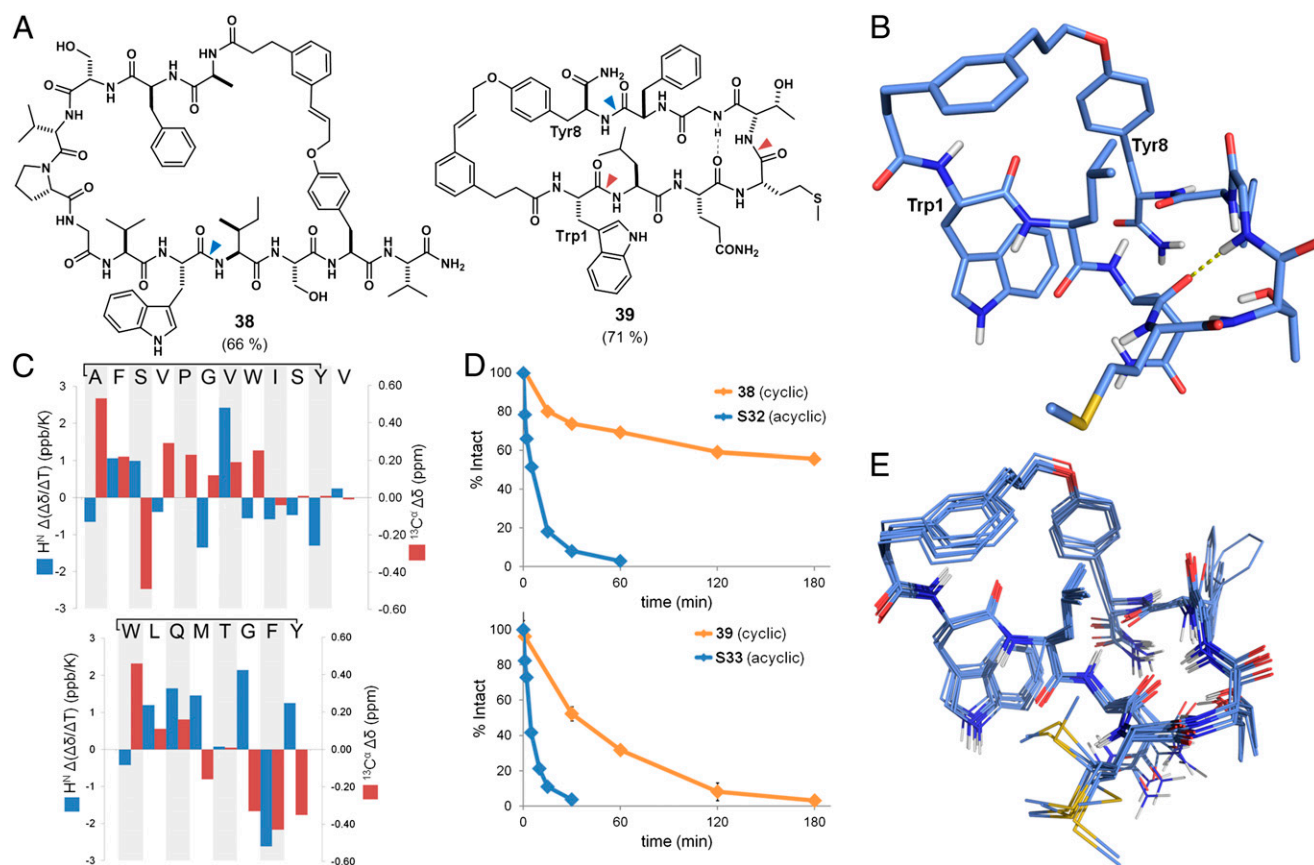


Fig. 5. Conformational analysis and proteolytic stability of **38** and **39**. (A) Planar structures of macrocycles **38** and **39**. Hydrogen bond $\text{H}^N\text{Gly}^6\text{-Gln}^3$ in **39** was inferred from analysis of backbone amide chemical shift temperature dependence. Blue triangle, denotes primary α -chymotrypsin cleavage site; magenta triangle, denotes secondary cleavage sites. (B) Lowest energy conformation of compound **39** determined from NMR analyses in $\text{DMSO-}d_6\text{:H}_2\text{O}$ (9:1). (C) Comparison of NMR metrics for backbone amide solvent exposure ($\text{H}^N \Delta(\Delta\delta/\Delta T)_{\text{cyclic-linear}}$) and backbone conformation ($^{13}\text{C}^\alpha \Delta\delta_{\text{cyclic-linear}}$) between macrocycles **38** (Upper), **39** (Lower), and their respective linear precursors **S32** and **S33**. (D) Macrocycle **38** exhibited greater stability against proteolysis by α -chymotrypsin in comparison with **S32** (Upper). Analogous stability was observed for macrocycle **39** over **S33** (Lower). (E) Ensemble of 10 low-energy conformers of **39**. Core macrocycle rmsd = 0.36 Å.

independently with **1**, which selectively acylated their amino termini. Exposure of the products to 5 mol % $\text{Pd}(\text{PPh}_3)_4$ rapidly formed macrocyclic aryl amines **37** and **30** in high yield (Fig. 4 and Table 2).

Longer Sequences Undergo Efficient Macrocyclization. Nascent secondary structure elements in longer peptides can assist or hinder cyclization attempts, depending upon how they influence access to the transition state for intramolecular reaction. Hindrance is common, and oligomeric by-products often form as a result (66, 67). High dilution (78), pseudodilution on solid-support (79), and conformationally restrained pseudoproline (80, 81) are used to improve cyclization efficiency. Techniques such as helical peptide “stapling,” based on ring-closing olefin metathesis, require folding of the helical element for efficient cyclization (82). To begin testing the utility of palladium π -allyl chemistry for cyclizing longer sequences, we prepared octa- and dodecapeptides WLQMTGFY and AFSVPGVWISYV. Acylation of these materials with template **1** followed by treatment of the products with 5 mol % $\text{Pd}(\text{PPh}_3)_4$ gave macrocyclic cinnamyl ethers **39** and **38**, respectively. As observed for shorter sequences, the cyclization reactions were efficient at room temperature and complete within 1 h. The 38- and 47-membered ring products were readily isolated by preparative HPLC and characterized. Competing dimerization or oligomerization was not observed.

These impressive results prompted us to investigate whether we had inadvertently chosen sequences poised to cyclize. Both **38** and **39** harbor potential turn-inducing motifs centered at proline

and glycine, respectively, which may accelerate the rate of ring closure. To explore this possibility, we used NMR to probe conformational preferences of macrocycles **38** and **39** relative to their linear precursors **S32** and **S33** (83, 84). Comparison of $^{13}\text{C}^\alpha$ shifts, expressed as $\Delta\delta_{\text{cyclic-linear}}$ in Fig. 5 C and E, revealed distinct differences in the backbone conformations of linear and cyclic structures (85, 86). These data imply that the linear precursors do not tightly occupy a product-like conformation, but perhaps sample an ensemble of states under these conditions. Differences were further evidenced by changes in the temperature dependence of backbone H^N chemical shifts following cyclization (87, 88). Notably, Val⁷ and Gly⁶ in macrocycles **38** and **39**, respectively, showed a temperature dependence of greater than -3 ppb/K, suggestive of internal hydrogen bonding at these positions (83, 89). Similar interactions were not observed in the linear precursors, wherein a smaller temperature dependence was measured at the same positions; these comparisons are illustrated in Fig. 5C as $\Delta(\Delta\delta/\Delta T)_{\text{cyclic-linear}}$. It appears that a product-like conformation of the linear precursor need not predominate in order for the palladium-catalyzed cyclization to occur.

Template 1 Stabilizes Secondary Structure and Enhances Proteolytic Stability in Vitro. Based on NMR evidence for internal hydrogen bonding, we next examined whether templated macrocycle **39** exhibited a defined conformation in solution. Complete resonance annotations from NMR spectra acquired in 9:1 $\text{DMSO-}d_6\text{:H}_2\text{O}$ –facilitated assignment of 80 intramolecular NOEs and 13 dihedral

angle restraints. Sequential H^N NOEs within the triad Met⁴-Thr-Gly⁶ indicated the presence of a beta turn. Transannular NOEs between Leu² and Phe⁷, and between Gln³ and the C terminus were indicative of the ring structure. Distance- and angle-constrained molecular mechanics calculations identified a tight ensemble of low energy conformers. The global energy minimum and an overlay of conformers of similar energy are shown Fig. 5 A and B. The region Gln³-Met-Thr-Gly-Phe⁷ occupies a type I β -turn, consistent with the observed Gly⁶ H^N temperature coefficient (−2.4 ppb/K). These data indicate a well-ordered core macrocycle and stabilization of the peptide domain, despite potential flexibility of the template.

Restricted conformational mobility is one means by which folded polypeptides evade enzymatic degradation (33, 90, 91). Accordingly, we examined the extent to which macrocycles **38** and **39** were protected against proteolytic degradation by α -chymotrypsin in vitro. As expected, linear compound **S33** was degraded rapidly, with primary cleavage occurring between Phe⁷ and Tyr⁸. Corresponding macrocycle **39** was 8.7-fold more stable in this assay (Fig. 5D) and was cleaved at the same site. Macrocycle **38** also exhibited resistance to proteolysis although product inhibition precluded accurate determination of its half-life and comparison with linear counterpart **S32**. Enzymatic hydrolysis between Trp⁸ and Ile⁹ was invariant between cyclic **38** and the linear material. These preliminary results are encouraging and imply that enhanced proteolytic stability observed for conventional cyclic peptides will be a feature of macrocycles derived from template **1** as well.

Conclusions

We have described methods to convert unmodified, unprotected linear peptides directly to stable macrocycles using **1** as a scaffold. Nonnatural amino acids are not required. The catalyzed ring-forming reaction is uniquely versatile and operates independent

of product ring size and composition. Side chain functional groups present in tyrosine, histidine, glutamic acid, and aspartic acid participate in the cyclization, as do a free carboxyl or amino terminus under appropriate conditions. Alcohols, guanidines, carboxamides, and thioethers neither participate nor interfere with the catalysis. The chemistry is well-suited to probe consensus peptide binding sites, to generate peptide-based positive controls for assay development, to stabilize and protect elements of secondary structure (i.e., turns, helices), and to create prototype leads for medicinal chemistry programs targeting protein/protein interactions. Simple procedures, mild reaction conditions, high yields, and tunable chemoselectivity provide for myriad possibilities. The chemistry compares favorably with other methods for peptide cyclization. The ready availability of peptides commercially will hopefully facilitate additional research by others. Lastly, we note that the bioorthogonal nature of the palladium catalysis may also allow integration with powerful combinatorial biology screens. We are happy to provide samples of template **1** to assist experimentation along these lines.

Materials and Methods

Peptides were prepared using standard Fmoc solid phase peptide synthesis protocols. Detailed synthetic procedures for the acylation of synthetic peptides with template **1** and Pd-catalyzed macrocyclization are available in the *SI Appendix*. Spectroscopic characterization of all previously undescribed compounds, proteolysis assay conditions, and details of the NMR solution structure of **39** are also available in the *SI Appendix*.

ACKNOWLEDGMENTS. We thank Dr. Robert Peterson for expert assistance in obtaining NMR correlation spectra, Albert Chan for helpful discussions, and Dr. Joseph Loo and Dr. Huilin Li for tandem mass spectra. Funding was provided by National Cancer Institute Grant P01 CA95471, the Donald J. and Jane M. Cram Endowment, National Science Foundation Graduate Research Fellowship DGE-0707424 (to T.E.R.), and National Science Foundation Major Instrumentation Grant CHE-1048804.

- Chène P (2006) Drugs targeting protein-protein interactions. *ChemMedChem* 1(4):400–411.
- Berg T (2008) Small-molecule inhibitors of protein-protein interactions. *Curr Opin Drug Discov Devel* 11(5):666–674.
- Arkin MR, Wells JA (2004) Small-molecule inhibitors of protein-protein interactions: Progressing towards the dream. *Nat Rev Drug Discov* 3(4):301–317.
- Souroujon MC, Mochly-Rosen D (1998) Peptide modulators of protein-protein interactions in intracellular signaling. *Nat Biotechnol* 16(10):919–924.
- DeLano WL, Ultsch MH, de Vos AM, Wells JA (2000) Convergent solutions to binding at a protein-protein interface. *Science* 287(5456):1279–1283.
- Zha J, Harada H, Yang E, Jockel J, Korsmeyer SJ (1996) Serine phosphorylation of death agonist BAD in response to survival factor results in binding to 14-3-3 not BCL-X (L). *Cell* 87(4):619–628.
- Macintosh C (2004) Dynamic interactions between 14-3-3 proteins and phosphoproteins regulate diverse cellular processes. *Biochem J* 381(Pt 2):329–342.
- Cochran AG (2000) Antagonists of protein-protein interactions. *Chem Biol* 7(4):R85–R94.
- Lu L, Arakaki AK, Lu H, Skolnick J (2003) Multimeric threading-based prediction of protein-protein interactions on a genomic scale: Application to the *Saccharomyces cerevisiae* proteome. *Genome Res* 13(6A):1146–1154.
- Davey NE, Edwards RJ, Shields DC (2007) The SLiMDisc server: Short, linear motif discovery in proteins. *Nucleic Acids Res* 35(Web Server issue):W455–9.
- Edwards RJ, Davey NE, Shields DC (2007) SLiMfinder: A probabilistic method for identifying over-represented, convergently evolved, short linear motifs in proteins. *PLoS ONE* 2(10):e967.
- Neduvu V, Russell RB (2006) Peptides mediating interaction networks: New leads at last. *Curr Opin Biotechnol* 17(5):465–471.
- Davey NE, et al. (2012) Attributes of short linear motifs. *Mol Biosyst* 8(1):268–281.
- Ahrens VM, Bellmann-Sickert K, Beck-Sickinger AG (2012) Peptides and peptide conjugates: Therapeutics on the upward path. *Future Med Chem* 4(12):1567–1586.
- Pillutla RC, et al. (2002) Peptides identify the critical hotspots involved in the biological activation of the insulin receptor. *J Biol Chem* 277(25):22590–22594.
- Bogan AA, Thorn KS (1998) Anatomy of hot spots in protein interfaces. *J Mol Biol* 280(1):1–9.
- Wells JA, McClendon CL (2007) Reaching for high-hanging fruit in drug discovery at protein-protein interfaces. *Nature* 450(7172):1001–1009.
- Moreira IS, Fernandes PA, Ramos MJ (2007) Hot spots—a review of the protein-protein interface determinant amino-acid residues. *Proteins* 68(4):803–812.
- Wilson AJ (2009) Inhibition of protein-protein interactions using designed molecules. *Chem Soc Rev* 38(12):3289–3300.
- Groner B, ed (2009) *Peptides as Drugs: Discovery and Development* (Wiley-VCH, Weinheim, Germany), pp xv, 226.
- Sehgal A (2002) Recent developments in peptide-based cancer therapeutics. *Curr Opin Drug Discov Devel* 5(2):245–250.
- Vally M, Seenu S, Pillarisetti S (2006) Emerging peptide therapeutics for inflammatory diseases. *Curr Pharm Biotechnol* 7(4):241–246.
- Vlieghe P, Lisowski V, Martinez J, Khrestchatsky M (2010) Synthetic therapeutic peptides: Science and market. *Drug Discov Today* 15(1–2):40–56.
- White CJ, Yudin AK (2011) Contemporary strategies for peptide macrocyclization. *Nat Chem* 3(7):509–524.
- Deber CM, Madison V, Blout ER (1976) Why cyclic peptides: Complementary approaches to conformations. *Acc Chem Res* 9(3):106–113.
- Marsault E, Peterson ML (2011) Macrocycles are great cycles: Applications, opportunities, and challenges of synthetic macrocycles in drug discovery. *J Med Chem* 54(7):1961–2004.
- Driggers EM, Hale SP, Lee J, Terrett NK (2008) The exploration of macrocycles for drug discovery—an underexploited structural class. *Nat Rev Drug Discov* 7(7):608–624.
- Kawakami T, et al. (2009) Diverse backbone-cyclized peptides via codon reprogramming. *Nat Chem Biol* 5(12):888–890.
- Gartner ZJ, et al. (2004) DNA-templated organic synthesis and selection of a library of macrocycles. *Science* 305(5690):1601–1605.
- Heinis C, Rutherford T, Freund S, Winter G (2009) Phage-encoded combinatorial chemical libraries based on bicyclic peptides. *Nat Chem Biol* 5(7):502–507.
- Smith JM, Vitali F, Archer SA, Fasan R (2011) Modular assembly of macrocyclic organo-peptide hybrids using synthetic and genetically encoded precursors. *Angew Chem Int Ed Engl* 50(22):5075–5080.
- Ng S, Jafari MR, Derda R (2012) Bacteriophages and viruses as a support for organic synthesis and combinatorial chemistry. *ACS Chem Biol* 7(1):123–138.
- Bird GH, et al. (2010) Hydrocarbon double-stapling remedies the proteolytic instability of a lengthy peptide therapeutic. *Proc Natl Acad Sci USA* 107(32):14093–14098.
- Davies JS (2003) The cyclization of peptides and decapeptides. *J Pept Sci* 9(8):471–501.
- Thakkar A, Trinh TB, Pei D (2013) Global analysis of peptide cyclization efficiency. *ACS Comb Sci* 15(2):120–129.
- Montalbetti CAGN, Falque V (2005) Amide bond formation and peptide coupling. *Tetrahedron* 61(46):10827–10852.
- Jackson DY, King DS, Chmielewski J, Singh S, Schultz PG (1991) General approach to the synthesis of short α -helical peptides. *J Am Chem Soc* 113(24):9391–9392.
- Giebel LB, et al. (1995) Screening of cyclic peptide phage libraries identifies ligands that bind streptavidin with high affinities. *Biochemistry* 34(47):15430–15435.
- Blackwell HE, Grubbs RH (1998) Highly efficient synthesis of covalently cross-linked peptide helices by ring-closing metathesis. *Angew Chem Int Ed* 37(23):3281–3284.

40. Jacobsen O, et al. (2011) Stapling of a 3(10)-helix with click chemistry. *J Org Chem* 76(5):1228–1238.
41. Peheré AD, Abell AD (2012) New β -strand templates constrained by Huisgen cycloaddition. *Org Lett* 14(5):1330–1333.
42. Chouhan G, James K (2011) CuAAC macrocyclization: High intramolecular selectivity through the use of copper-tris(triazole) ligand complexes. *Org Lett* 13(10):2754–2757.
43. Kates SA, et al. (1993) A novel, convenient, 3-dimensional orthogonal strategy for solid-phase synthesis of cyclic-peptides. *Tetrahedron Lett* 34(10):1549–1552.
44. Lundquist JT, 4th, Pelletier JC (2002) A new tri-orthogonal strategy for peptide cyclization. *Org Lett* 4(19):3219–3221.
45. Schmidt U, Langner J (1997) Cyclotetrapeptides and cyclopentapeptides: Occurrence and synthesis. *J Pept Res* 49(1):67–73.
46. Jackson S, et al. (1994) Template-constrained cyclic peptides: Design of high-affinity ligands for GPIIb/IIIa. *J Am Chem Soc* 116(8):3220–3230.
47. Boger DL, Myers JB (1991) Design and synthesis of a conformational analog of deoxybouvardin. *J Org Chem* 56(18):5385–5390.
48. Marsault E, et al. (2008) Efficient parallel synthesis of macrocyclic peptidomimetics. *Bioorg Med Chem Lett* 18(16):4731–4735.
49. Ernest I, Kalvoda J, Rihs G, Mutter M (1990) Three novel mimics for the construction of sterically constrained protein turn models. *Tetrahedron Lett* 31(28):4011–4014.
50. Cheng RP, Suich DJ, Cheng H, Roder H, DeGrado WF (2001) Template-constrained somatostatin analogues: A biphenyl linker induces a type-V' turn. *J Am Chem Soc* 123(50):12710–12711.
51. Zhao HD, et al. (2008) Acid promoted cinnamyl ion mobility within peptide derived macrocycles. *J Am Chem Soc* 130(42):13864–13866.
52. Wei Q, Harran S, Harran PG (2003) Methods to initiate synthetic re-structuring of peptides. *Tetrahedron* 59(45):8947–8954.
53. Lawson KV, Rose TE, Harran PG (2011) Synthesis of a designed sesquiterpenoid that forms useful composites with peptides and related oligomers. *Tetrahedron Lett* 52(6): 653–654.
54. Lawson KV, Rose TE, Harran PG (2013) Template-induced macrocycle diversity through large ring-forming alkylations of tryptophan. *Tetrahedron* 69(36):7683–7691.
55. Trost BM, Zhang T, Sieber JD (2010) Catalytic asymmetric allylic alkylation employing heteroatom nucleophiles: A powerful method for C-X bond formation. *Chem Sci* 1(4): 427–440.
56. Trost BM (2004) Asymmetric allylic alkylation, an enabling methodology. *J Org Chem* 69(18):5813–5837.
57. Fürstner A, Weintritt H (1998) Total synthesis of roseophilin. *J Am Chem Soc* 120(12): 2817–2825.
58. Fürstner A, Krause H (1999) Flexible synthesis of metacycloprodigiosin and functional derivatives thereof. *J Org Chem* 64(22):8281–8286.
59. Trost BM, Ohmori M, Boyd SA, Okawara H, Brickner SJ (1989) Palladium-catalyzed synthesis of macrocycles. A total synthesis of (-)-aspothalasin B. *J Am Chem Soc* 111(21):8281–8284.
60. Trost BM, Verhoeven TR (1980) Cyclization catalyzed by palladium(0). Initial studies and macrolide formation. *J Am Chem Soc* 102(14):4743–4763.
61. Evans LA, et al. (2008) Counterintuitive kinetics in Tsuji-Trost allylation: Ion-pair partitioning and implications for asymmetric catalysis. *J Am Chem Soc* 130(44): 14471–14473.
62. Trost BM, Bunt RC (1993) On the nature of the ion pair as a nucleophile in Pd catalyzed alkylations with dieny carboxylates. *Tetrahedron Lett* 34(47):7513–7516.
63. Rotstein BH, Rai V, Hili R, Yudin AK (2010) Synthesis of peptide macrocycles using unprotected amino aldehydes. *Nat Protoc* 5(11):1813–1822.
64. Hili R, Rai V, Yudin AK (2010) Macrocyclization of linear peptides enabled by amphoteric molecules. *J Am Chem Soc* 132(9):2889–2891.
65. Londregan AT, Farley KA, Limberakis C, Mullins PB, Piotrowski DW (2012) A new and useful method for the macrocyclization of linear peptides. *Org Lett* 14(11):2890–2893.
66. Jagasia R, Holub JM, Bollinger M, Kirshenbaum K, Finn MG (2009) Peptide cyclization and cyclodimerization by Cu(I)-mediated azide-alkyne cycloaddition. *J Org Chem* 74(8):2964–2974.
67. Punna S, Kuzelka J, Wang Q, Finn MG (2005) Head-to-tail peptide cyclodimerization by copper-catalyzed azide-alkyne cycloaddition. *Angew Chem Int Ed Engl* 44(15): 2215–2220.
68. Collins JC, James K (2012) Emac: A comparative index for the assessment of macrocyclization efficiency. *Med Chem Comm* 3(12):1489–1495.
69. Pneumatikakis G, Chassapis C, Rontoyianni A (1993) Complexes of palladium(II) chloride with histidine methylester, X-ray crystal structure of Pd(HisOMe)Cl₂. Ternary complexes of palladium(II) with histidine methylester and nucleosides. *J Inorg Biochem* 49(2):83–96.
70. L. Best S, et al. (1997) Gold(III) and palladium(II) complexes of glycyglycyl-L-histidine: Crystal structures of [Au^{III}(Gly-Gly-L-His-H₂)]Cl \cdot H₂O and [Pd^{II}(Gly-Gly-L-His-H₂)] \cdot 1.5H₂O and HisNH deprotonation. *J Chem Soc Dalt Trans* (15):2587–2596.
71. Pitner TP, Wilson EW, Martin RB (1972) Properties of palladium(II) complexes of peptides and histidine in basic solutions. *Inorg Chem* 11(4):738–742.
72. Klingensmith LM, Strieter ER, Barder TE, Buchwald SL (2006) New insights into Xantphos/Pd-catalyzed C-N bond forming reactions: A structural and kinetic study. *Organometallics* 25(1):82–91.
73. Collins JC, et al. (2012) Macrocyclizations for medicinal chemistry: Synthesis of druglike macrocycles by high-concentration Ullmann coupling. *J Org Chem* 77(24):11079–11090.
74. Dijkstra G, Kruizinga WH, Kellogg RM (1987) An assessment of the causes of the "cesium effect". *J Org Chem* 52(19):4230–4234.
75. Trost BM, Cossy J (1982) Palladium-mediated macroheterocyclization. A synthesis of inandenin-12-one. *J Am Chem Soc* 104(24):6881–6882.
76. Mattern IE, Pittard J (1971) Regulation of tyrosine biosynthesis in *Escherichia coli* K-12: Isolation and characterization of operator mutants. *J Bacteriol* 107(1):8–15.
77. Geurink PP, et al. (2013) Incorporation of non-natural amino acids improves cell permeability and potency of specific inhibitors of proteasome trypsin-like sites. *J Med Chem* 56(3):1262–1275.
78. Malesevic M, Strijowski U, Bächle D, Sewald N (2004) An improved method for the solution cyclization of peptides under pseudo-high dilution conditions. *J Biotechnol* 112(1–2):73–77.
79. Scott LT, Rebek J, Ovsyanko L, Sims CL (1977) Organic chemistry on the solid phase. Site-site interactions on functionalized polystyrene. *J Am Chem Soc* 99(2):625–626.
80. Botti P, Pallin TD, Tam JP (1996) Cyclic peptides from linear unprotected peptide precursors through thiazolidine formation. *J Am Chem Soc* 118(42):10018–10024.
81. Wöhr T, et al. (1996) Pseudo-prolines as a solubilizing, structure-disrupting protection technique in peptide synthesis. *J Am Chem Soc* 118(39):9218–9227.
82. Kim Y-W, Grossmann TN, Verdine GL (2011) Synthesis of all-hydrocarbon stapled α -helical peptides by ring-closing olefin metathesis. *Nat Protoc* 6(6):761–771.
83. Kessler H (1982) Conformation and biological activity of cyclic peptides. *Angew Chem Int Ed Engl* 21(7):512–523.
84. Wüthrich K (1976) *NMR in Biological Research: Peptides and Proteins* (American Elsevier, Amsterdam).
85. Saitō H (1986) Conformation-dependent ¹³C chemical shifts: A new means of conformational characterization as obtained by high-resolution solid-state ¹³C NMR. *Magn Reson Chem* 24(10):835–852.
86. Wishart DS, Sykes BD, Richards FM (1991) Relationship between nuclear magnetic resonance chemical shift and protein secondary structure. *J Mol Biol* 222(2):311–333.
87. Cierpicki T, Otlewski J (2001) Amide proton temperature coefficients as hydrogen bond indicators in proteins. *J Biomol NMR* 21(3):249–261.
88. Baxter NJ, Williamson MP (1997) Temperature dependence of ¹H chemical shifts in proteins. *J Biomol NMR* 9(4):359–369.
89. Bara YA, Friedrich A, Kessler H, Molter M (1978) Peptidkonformationen. II: ¹H-NMR-Untersuchungen zur Konformation von cyclo-(Phe₃Gly₂). *Chem Ber* 111(3):1045–1057.
90. Rozek A, Powers J-PS, Friedrich CL, Hancock REW (2003) Structure-based design of an indolicidin peptide analogue with increased protease stability. *Biochemistry* 42(48): 14130–14138.
91. Gentilucci L, De Marco R, Cerisoli L (2010) Chemical modifications designed to improve peptide stability: Incorporation of non-natural amino acids, pseudo-peptide bonds, and cyclization. *Curr Pharm Des* 16(28):3185–3203.